Rheological Characteristics and Morphologies of Styrene–Butadiene–Maleic Anhydride Block Copolymers

Wanjie Wang, Chunhui Li, Yanxia Cao, Jinzhou Chen, Jingwu Wang

College of Materials Science and Engineering, Zhengzhou University, Zhengzhou 450052, China

Received 2 February 2010; accepted 2 May 2010
DOI 10.1002/app.34606
Published online 7 September 2011 in Wiley Online Library (wileyonlinelibrary.com).

ABSTRACT: Studies on the morphologies and rheological characteristics of two styrene–butadiene–maleic anhydride block copolymers (SBMa) have been performed. The transmission electron microscopy micrographs show that the morphologies of SBMa change from matrix–island structure to co-continuous structure. Curves for dynamic modulus varied with frequency (ω) show obvious solid-like behavior in the low ω region, which is typical for ordered block copolymers or networked materials. Van Gurp–Palmen plots have been used to exploit the thermorheological complexity of two copolymers. The master curves of two copolymers have been acquired through time–temperature superposition principle, and the plateau modulus (G_N^0) have been obtained from G' at ω, where the loss tangent (tan δ) approaches a minimum. Meanwhile, Williams–Landel–Ferry equation has been used to evaluate the free volume parameters. The relaxation time spectra of two copolymers have been calculated and fitted with modified Baumgaertel–Schausberger–Winter model. J Appl Polym Sci 123: 3234–3241, 2012

Key words: morphology; rheology; Van Gurp–Palmen plots; mBSW model

INTRODUCTION

Introducing a compatibilizer is an effective way to achieve good compatibilization for immiscible blends. Generally, block, graft, and random copolymer with reactive functional groups are usually used as an effective compatibilizer to reduce the interface tension between immiscible components and obtain the polymer blends with good mechanical properties.[1,2] The styrene block copolymers (styrene–butadiene–styrene copolymer, styrene–isoprene–styrene copolymer [SIS], and styrene–ethylene–butylene–styrene copolymer) are an important kind of compatibilizer to improve the compatibilization of immiscible blends.[3–5] To obtain good compatibilization, it is necessary to investigation the viscoelastic behavior of compatibilizer because rheological measurements provide an effective approach to characterize the structures and properties of polymer materials.[6,7]

The viscoelastic behaviors of the styrene block copolymers are related closely with block components and their morphologies and have attracted ever-increasing interest of researches. Yoshida and Christian[8] reported the rheological behavior of hydrogenated styrene–butadiene copolymers (HSBC). The entanglement molecular weights (M_e) calculated for HSBC with 49.5–68.9 wt % styrene blocks are 2380–3270 g/mol, which is closed to that of polyethylene, and M_e depends on temperature. Chen et al.[9–11] reported the creep and relaxation behaviors of ethylene–styrene block copolymer in the glass transition region. The linear and large amplitude stress relaxation measurements show the complex relaxation behaviors, which are related closely to molecular structure. The plateau modulus of blend composed of block copolymer and polyethylene is corresponding to the volume mixing equation. Widmaier et al.[12] investigated the dependence of microstructure of SIS on temperature. SIS block copolymer shows lamellar structure and has high molecular weight. The long range order structure is destroyed when the temperature increased, which can be exhibited obviously by the melting rheological behavior. The order–disorder temperature (T_{ODT}) is approximately 225°C, which is also investigated by other authors. Stangler and Abetz reported the orientation behaviors of styrene–isoprene and styrene–isoprene–methyl methacrylate block copolymers under large amplitude oscillatory shear.[13] The results show that diblock copolymer can orient along the perpendicular and parallel directions but triblock copolymer only along perpendicular direction. The analysis of dynamic rheology demonstrates that shear can accelerate the microphase separation of methyl methacrylate blocks. Thunga et al.[14] reported the influence of molecular architecture of S-S/B-S

Correspondence to: W. Wang (wwj@zzu.edu.cn).
Contract grant sponsor: National Natural Science Foundation of China; contract grant number: 50903076.
Contract grant sponsor: China Postdoctoral Science Foundation; contract grant number: 20080440826.

TABLE I
The Molecular Characteristics of Two Block Copolymers

Sample	PS/PB (weight ratio)	Maleic anhydride content (wt %)	MFI (g/10 min, 220°C × 10 kg)	M_n (g/mol)	M_w (g/mol)	PDI
SBMa1	55/15	10	5	37,900	86,700	2.290
SBMa2	45/15	7	3	23,400	83,000	3.547

triblock copolymers on rheological properties. The rheological properties are observed to be strongly influenced by the relative composition of the S-SB-S triblock copolymers. Increasing the S/B ratio from 1:1 to 1:2 in the middle block has lead to a change in morphology from wormlike to lamellar.

It can be seen that the styrene block copolymers show the complex viscoelastic behaviors, which is inevitable to influence the degree of compatibilization when the styrene block copolymers act as a kind of compatibilizer. Thus, the purpose of this article is to investigate the rheological characteristics of two new compatibilizers, styrene–butadiene–maleic anhydride (SBMa) triblock copolymers and discuss the influence of molecular parameters on the dynamic viscoelastic behaviors and relaxation behaviors.

EXPERIMENTAL

Materials

SBMa triblock copolymer was provided by Shanghai Sunny New Technology Development Co. (Shanghai, China). The information about two copolymers has been listed in Table I. The antioxidant (B215) was supplied by Ciba-Geigy Co., Switzerland. The relative molecular weight was 647, T_m = 453–458 K.

Preparation of samples

Copolymers and antioxidant were blended in a Haake torque rheometer (Rheoflixer Polylab) at 473 K for 3 min. The samples were compressedly molded at 200°C into disks of approximately 25 mm diameter and 1.2 mm thickness.

Dynamic rheological measurements

Melt rheological tests were conducted on an ARES Rheometer (Rheometrics, USA) in parallel plates oscillatory mode. The dynamic strain sweeps were performed from 0.01 to 100% to determine the linear viscoelastic region. The dynamic time sweep (the strain amplitude is 3%, the frequency amplitude is 1 rad/s, and the measure time is 3600 s) at different temperatures shows almost straight lines, demonstrating that the sample in the range of measure time is under equilibrum condition. The dynamic frequency sweep was from 0.01585 to 100 rad/s, the strain amplitude was maintained as 3% to ensure that rheological behavior is located in the linear viscoelastic region, and the test temperatures were 443, 453, 463, 473, 483, and 493 K.

Transmission electron microscopy

Transmission electron microscopy (TEM) was performed in the bright-field mode on a Tecnai G220 transmission electron microscope operating at 200 kV. Ultrathin sections of the block copolymers were obtained using an RMC ultramicrotome equipped with a diamond knife. The rigidity of the samples was sufficient to prepare high-quality ultrathin sections at room temperature. The ultrathin sections were picked on copper grids and stained using gaseous osmium tetroxide (OsO_4) reacting preferentially with polybutadiene (PB) in the SBMa sample.

RESULTS AND DISCUSSIONS

Morphologies of SBMa copolymers

Figure 1 shows the TEM micrographs of SBMa1 sample stained with OsO_4. In the case of staining with OsO_4, the polystrene (PS) phase appears gray on the TEM micrograph, the PB phase is dark, and the maleic anhydride (MA) phase is white. It can be seen that the PB phases disperse in the PS phases and exhibit irregular shapes, showing the character of microseparation phase structure. The sizes of PB phases are less than 1 μm. The TEM micrograph with higher magnifications shows that the MA phases disperse with good distribution in the PB phases and the shapes of MA phases are spherical or elliptical. With the PB content increasing, the PB phases agglomerate gradually and form the bigger phases (Fig. 2). The morphologies of SBMa have a transition from matrix–island structure to co-continuous structure. However, MA phases of SBMa2 still keep the spherical or elliptical morphologies, but the sizes of MA phases enlarge with the MA content increasing. The complex morphologies of two samples should be attributed to the thermodynamic compatibility of blocks and polydispersity.

Dependence of viscoelastic behaviors on frequency and temperature

Figure 3 shows frequency dependence of dynamic storage modulus (G'), dynamic loss modulus (G''),

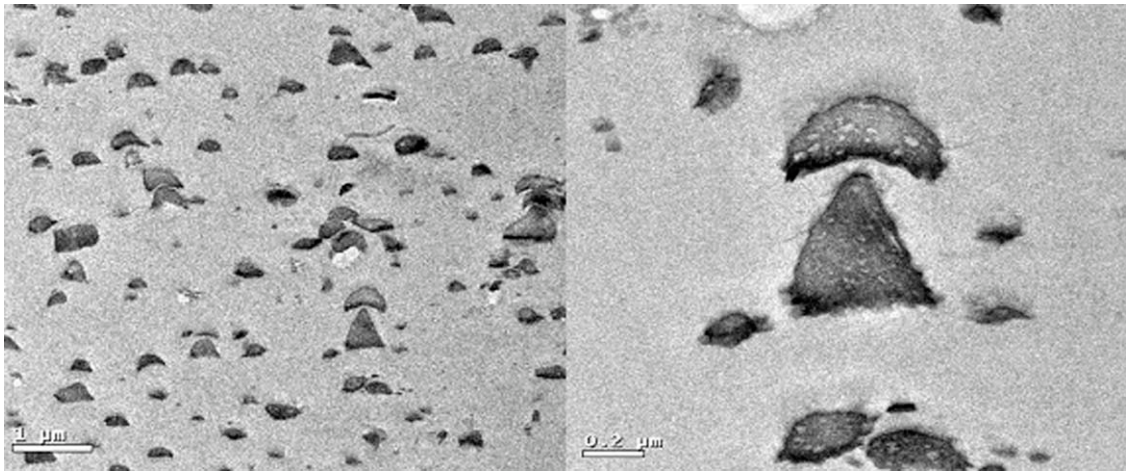

Figure 1 TEM micrographs of SBMa1 sample stained with osmium tetroxide.

and phase angle (δ) for two block copolymers at 473 K. It can be seen that the viscoelastic behaviors of two block copolymers show some deviation from those of homopolymers in the low frequency (ω) region (i.e., $G' \propto \omega^2$, $G'' \propto \omega$ at low ω).[15] As for SBMa2, the slopes of G' and G'' curves in the low ω region are 1.19 and 1.23. The G' and G'' curves show two intersections, where δ passes through 45°. One critical frequency is 2.52 rad/s, showing an obvious transition from solid-like viscoelastic behavior to liquid-like behavior; the other one is 0.32 rad/s, exhibiting another transition from liquid-like behavior to solid-like viscoelastic behavior. Between these critical frequencies, G' and G'' enclose a lens-shaped region, and its greatest separation is corresponding to a maximum in the phase angle ($\delta_{max} = 47.3°$). This low-frequency solid-like behavior is typical for ordered block copolymers or networked materials where structure interferes with large-scale relaxation.[16–18] SBMa1 exhibits similar curves in shape, but the separation of G' and G'' between the two critical frequencies ($\omega_c = 4.98$ rad/s and $\omega_c = 0.12$ rad/s) is high, and δ_{max} is 49.4° higher than that of SBMa2, consistent with its higher molecular weight. However, the dependence of G' and G'' on ω is almost equivalent. These differences are attributed to the relative low molecular weight and high polydispersity index of SBMa2.

Figure 4 shows G' and G'' curves for two copolymers at 463, 473, and 483 K. G' and G'' curves of two copolymers for three temperatures show two intersections and seem merely shifted along the frequency axis as the temperature changes, indicating no change for ordering degree. However, it is noted that G' curves at 473 K for two copolymers exhibit a relatively obvious second plateau in the low ω region. In rheology, this phenomenon is believed to be responsible for the emergence of phase separation and the existence of ordered structures to some extent such as agglomeration, skeleton, network, etc. In addition, the molecular weight distribution is an important factor to affect the dynamic rheological behavior in terminal region.[19] In these cases, the polydispersity of copolymers is perhaps the main reason for the emergence of second plateau. The areas of a lens-shaped region increase with the temperature increasing, which is accompanied with the change of entropy and energy. Based on the

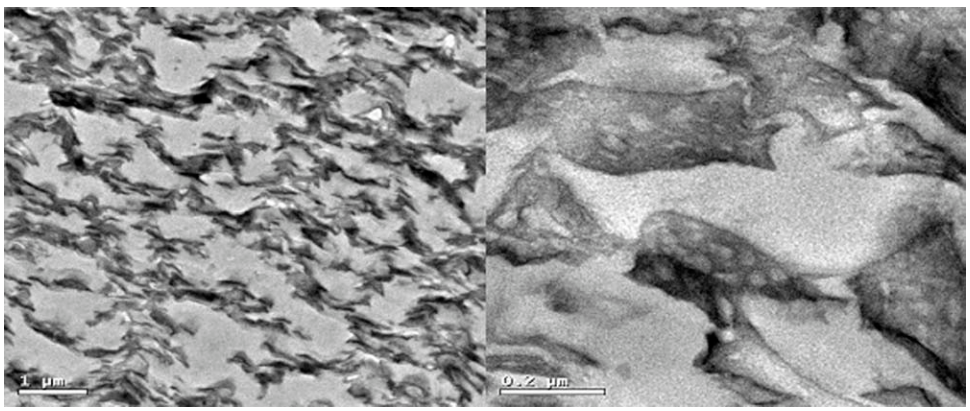

Figure 2 TEM micrographs of SBMa2 sample stained with osmium tetroxide.

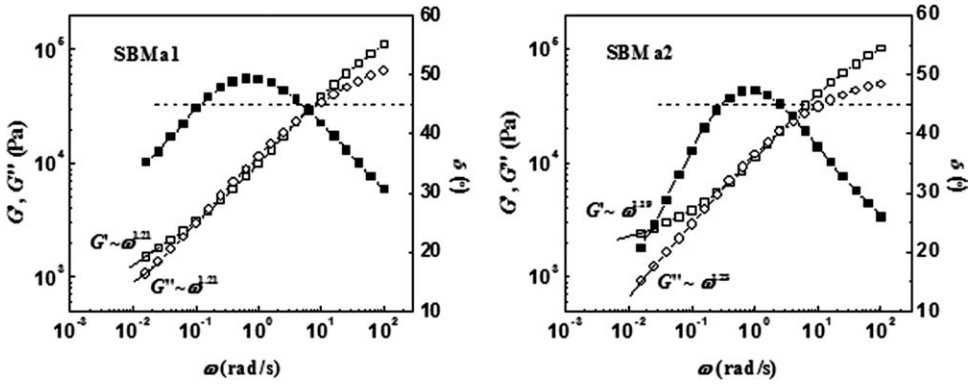

Figure 3 Frequency dependence of dynamic storage modulus G' (open square), dynamic loss modulus G'' (open circle), and phase angle δ (black square) at 473 K for two kinds of block copolymers.

molecular kinetic theory, the viscoelastic behaviors between the two crossovers are mainly controlled by the configurational rearrangement of relative short chain segment, but the entanglement and ordered structure with long relaxation time have little effect on these changes. In the low ω region, the topology restrains of entanglement have great effect on the change of long-range configuration. With the temperature increasing, the heat motion of macromolecules become strong, which weaken the topology restrains of entanglement and make the change of long-range configuration happen in the high ω.

Evaluation of viscoelastic behavior using Van Gurp–Palmen plots

To evaluate the more obvious dependence of the viscoelastic behavior on temperature, Van Gurp–Palmen plots have been used to exploit the thermorheological complexity.[20,21] In this method, the phase angle, ($\delta = \text{atan}(G''/G')$) of the measured dynamic rheological data is plotted against the corresponding absolute value of the shear complex modulus ($(|G^*| = (G'^2 + G''^2)^{1/2})$). Where the time–temperature superposition (TTS) principle holds, curves for different temperatures will overlap. However, when TTS does not hold (as generally to be expected in systems with phase segregation), this presentation facilitates comparison of data taken at different temperatures, free from any uncertainty associated with shifting curves along the frequency axis. Such plots have been applied in studies of polydispersity, blend miscibility and copolymers.[22–24]

Figure 5 shows Van Gurp–Palmen plots for two block copolymers. As for SBMa1, the curves of Van Gurp–Palmen plots exhibit maxima in δ, with clear superposition at higher and lower values of $|G^*|$ but less clean overlap at intermediate values. The slight shift in δ at these intermediate values is inferred to arise from gradual alignment of the block copolymer domains because little change is seen at lower values of $|G^*|$ to indicate the system is becoming less ordered. Furthermore, the δ values of peaks increase with the temperature increasing, which is consistent with this copolymer becoming less microphase segregated at higher temperature and thus displaying more liquid-like behavior. In addition, the curves at 493 and 443 K exhibit minima, which are corresponding to the first and second plateau moduli. Although the curves of SBMa2

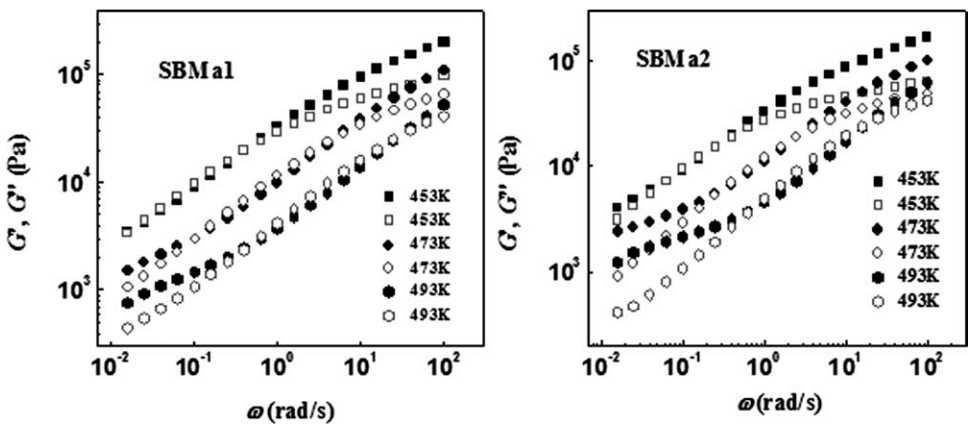

Figure 4 Frequency dependence of G' and G'' at various temperatures for two block copolymers.

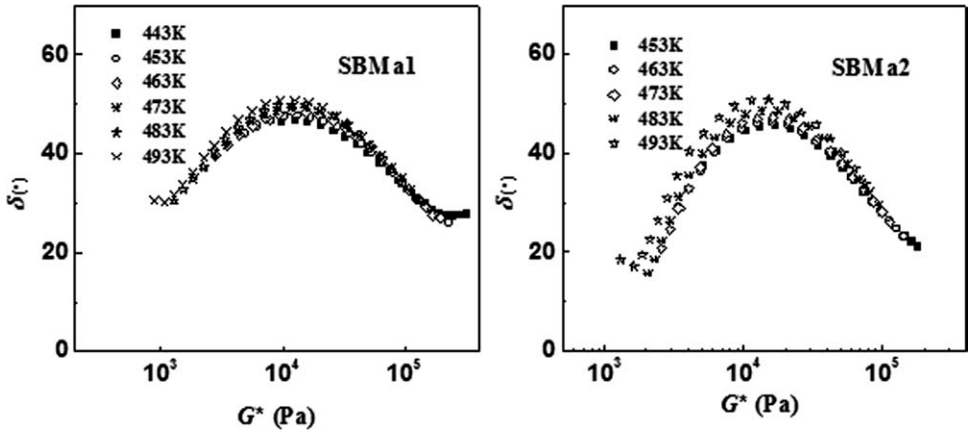

Figure 5 Van Gurp–Palmen plots for two block copolymers.

show similar change trend, it is noted that the curve of 493 K does not overlap completely with those of other temperatures at lower values of $|G^*|$, which can be attributed to the relatively wide molecular weight distribution.

Measurement and calculation of the plateau modulus G_N^0

It is well known that entanglement can be considered to be temporary or nonchemical crosslinks. According to the theory of rubber elasticity, the plateau modulus is defined by the following equation[15]:

$$G_N^0 = \frac{\rho RT}{M_e}, \tag{1}$$

where R is the gas constant, T is the absolute temperature, and M_e is entanglement molecular weight.

Taking the effects of chain slippage on entanglement into consideration, Doi–Edwards reptation theory gives[25]:

$$G_N^0 = \frac{4}{5}\frac{\rho RT}{M_e}. \tag{2}$$

The importance of G_N^0 for polymer physics is that it provides a direct way to measure the degree of entanglement in a polymer melt through above equation. The behavior of polymer melts in both the rubbery and terminal zones is strongly affected by M_e, and it has strong consequences on both viscous and elastic properties. M_e has also been reported to affect the micromechanisms of deformation (crazing and shear yielding) and the failure of polymers in the solid state.[26–30]

There are many methods to determine G_N^0 in different cases.[31–36] Usually, G_N^0 for amorphous polymer can be estimated from G' at ω, where the loss tangent (tan δ) approaches a minimum[31]:

$$G_N^0 = [G']_{\tan\delta \to \text{minimum}}. \tag{3}$$

Figure 6 shows the master curves of G' and G'' for two copolymers at the reference temperature of 473 K. The TTS based on the Williams–Landel–Ferry (WLF) equation was successfully applicable. Although the master curves extend for nearly six decades, there are no emergence of the obvious glass plateau and the terminal flow behavior because of the relatively narrow temperature windows. There

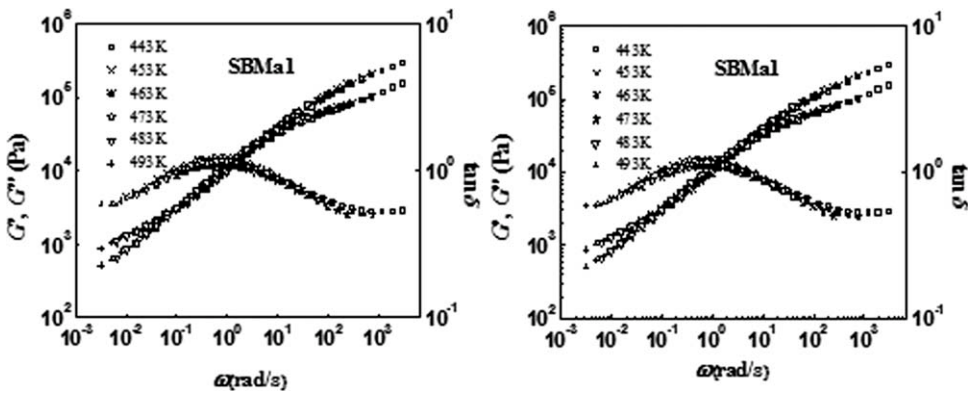

Figure 6 The master curves of two block copolymers at the reference temperature, $T_{ref} = 473$ K.

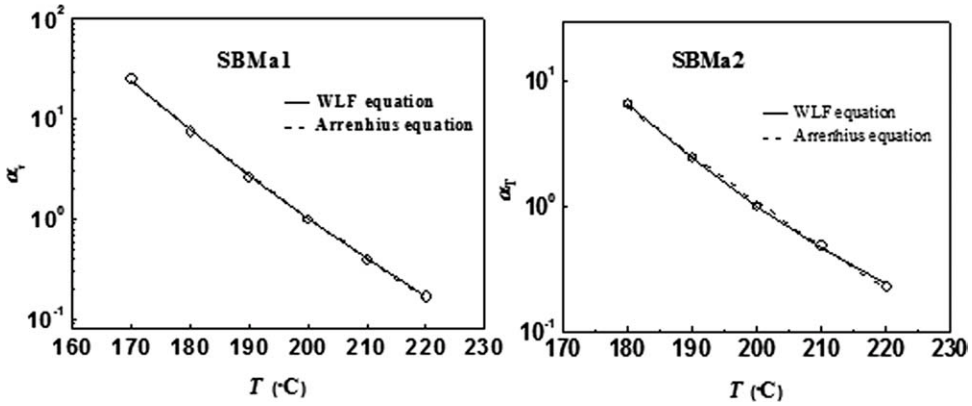

Figure 7 Relationship between horizontal shift factors (a_T) and temperature for two block copolymers and their fits using WLF and Arrhenius equations.

are minima in the tan δ curves for two copolymers; therefore, we can obtain the value of G_N^0 according to eq. (3). The process of determination is by the aid of the software of TA orchestrator (version V7.1).G_N^0 = 1541Pa (SBMa2), G_N^0 = 927 Pa (SBMa1). According to WLF equation, the shift factor a_T follows[37]:

$$\log a_T = \log \frac{\eta_0(T)}{\eta_0(T_{\text{ref}})} = \frac{-C_1(T - T_{\text{ref}})}{C_2 + (T - T_{\text{ref}})}, \quad (4)$$

where a_T is defined as the ratio of the viscosity at temperature T relative to the viscosity at the reference temperature T_{ref}, and C_1 and C_2 are empirical parameters. Two constants, C_1 and C_2, are obtained from the fit at the given reference temperature.

The C_1 and C_2 parameters are related to the free volume parameters α_f (the free volume thermal expansion coefficient) and f_0 (the fractional free volume at T_0), using the following equations[15]:

$$f_0 = B/2.303C_1, \quad (5)$$

$$\alpha_f = B/2.303C_1C_2, \quad (6)$$

where B is an empirical constant near unity. A typical plot of log a_T versus T fit to the WLF equation is shown in Figure 7 by solid line. The curves of a_T versus T can also be simulated by Arrhenius equation, and the results are demonstrated by the dotted line in Figure 7.

$$\ln a_T = \frac{E_a}{R}\left(\frac{1}{T} - \frac{1}{T_{\text{ref}}}\right). \quad (7)$$

It can be seen that both methods can describe well the variation of a_T with T, and the parameters obtained through simulation are listed in Table II. Compared with the parameters of two copolymers, SBMa2 exhibits the relatively high free volume fraction, free volume thermal expansion coefficient, and relatively low flow activation energy. The reasons for these are that SBMa2 has a relatively wide molecular weight distribution and the motions of macromolecular chains are difficult.

Determination and simulation of relaxation time spectrum

In general, real entanglement polymers exhibit a broad relaxation time spectrum because of the high flexibility and associated interaction of many polymer chains.

$$G'(\omega) = G_e + \int_{-\infty}^{+\infty} H(\tau)\omega^2\tau^2/(1 + \omega^2\tau^2)d\ \ln(\tau). \quad (8)$$

$$G''(\omega) = \int_{-\infty}^{+\infty} H(\tau)\omega\tau/(1 + \omega^2\tau^2)d\ \ln(\tau). \quad (9)$$

For uncrosslinked melts at $\tau = \infty$, the permanent elastic contribution G_e is 0. The terminal behavior for $\tau \to \infty$ and $\omega \to 0$ becomes clear from eqs. (8) and (9) and shows that $G''(\omega) \sim \omega'$, $G'(\omega) \sim \omega^2$. The calculation method of relaxation spectrum has been studied by many researchers, most are calculated by the aid of viscoelastic parameters (relaxation modulus $G(t)$, G', and G'') varied with time scales.[38–40]

TABLE II
WLF and Free Volume Parameters for Two Block Copolymers

Samples	C_1	C_2 (K)	$C_1 \cdot C_2$	f_0/B	$\alpha_f/B \times 10^4$ (K^{-1})	E_a (kJ/mol)
SBMa2	5.22	147.67	770.84	0.083	5.63	154.93
SBMa1	12.04	291.96	3515.2	0.036	1.24	181.56

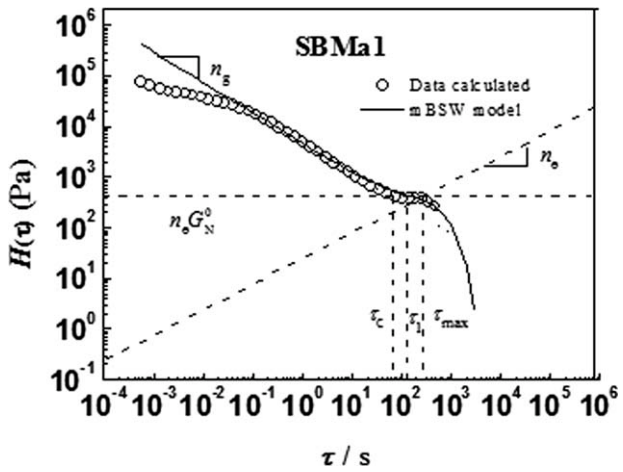

Figure 8 The relaxation time spectrum of SBMA1 and its fitting with the mBSW model.

$$H(\tau) = -G(t)\left[\frac{d\ \log G(t)}{d\ \log t} - \left(\frac{d\ \log G(t)}{d\ \log t}\right)^2 - \frac{1}{2.303}\frac{d^2\ \log G(t)}{d\ (\log t)^2}\right]\Bigg|_{t=2\tau,} \quad (10)$$

$$H(\tau) = G'\left[\frac{d\ \log G'}{d\ \log\omega} - \frac{1}{2}\left(\frac{d\ \log G'}{d\ \log\omega}\right)^2 - \frac{1}{4.606}\frac{d^2\ \log G'}{d\ (\log\omega)^2}\right]\Bigg|_{1/\omega=\tau/\sqrt{2}}, \quad (11)$$

$$H(\tau) = \frac{2}{\pi}\left[G'' + \frac{4dG''}{3d\ \ln\omega} + \frac{1}{3}\frac{d^2G''}{d(\ln\omega)^2}\right]\Bigg|_{1/\omega=\tau/\sqrt{5}}. \quad (12)$$

The above equations are acquired based on the second approximation method of viscoelastic parameters; the relationship between the relaxation time and measurement time and frequency should be understood. In these cases, we calculated the relaxation spectrums of two copolymers by using eq. (11).

Baumgaertel et al.[41] found that the relaxation spectrums of linear flexible polymers with molecules of uniform length can be well represented as:

$$H(\tau) = \begin{cases} n_eG_N^0\left[\left(\frac{\tau}{\tau_c}\right)^{-n_g} + \left(\frac{\tau}{\tau_{max}}\right)n_e\right], & \text{for } \tau \le \tau_{max} \\ 0 & \text{for } \tau > \tau_{max} \end{cases}, \quad (13)$$

where τ_{max} is the longest relaxation time, n_e and n_g are the slopes of the spectrum in the entanglement and short time scale zones, respectively, and τ_c is the time at the intersect within the short time scale region. The first term in the brackets of eq. (13) represents the high ω region, whereas the second term describes the entanglement and flow regions. Moreover, eq. (13) can describe the relaxation time spectrums for narrowly distributed polymers well; however, it appears more or less deviation for broadly distributed polymers. Accordingly, Baumgaertel and Winter[42] modified it and obtained

$$H(\lambda) = \left[H_g\left(\frac{\tau}{\tau_c}\right)^{-n_g} + n_eG_N^0\left(\frac{\tau}{\tau_{max}}\right)n_e\right]\exp[-\tau/\tau_{max}]^\beta, \quad (14)$$

where $H_g = n_eG_N^0(\tau_1/\tau_c)(\tau_1/\tau_{max})$, with τ_1 being the time at which the contribution from the short time scale and entanglement regions is the same, and β is the shape parameter. With β value increasing, eq. (14) gradually approaches eq. (13). Introducing exponential terms and comparing with eq. (13), we find that eq. (14) can describe relaxation time spectrum better, especially at terminal region.

Figures 8 and 9 show the relaxation spectrums of two copolymers and their fits by the modified Baumgaertel–Schausberger–Winter (mBSW) model. It can be seen that the relaxation curves have similar shape and show valleys in the long time region, and the whole relaxation spectrum can be divided into three regions (glass, entanglement, and terminal region). The exponent β controls the sharpness of the cutoff of the spectrum. With β value increasing, eq. (14) gradually approaches eq. (13). Because eq. (13) can describe the relaxation spectrum of narrowly distributed polymers well, it is believed that the β value can exhibit polydispersity of polymers. With β value increasing, the polydispersity index decreases. The parameters of mBSW for two copolymers have been listed in Table III. The results show that the β value of SBMa2 is lower than that of SBMa1, implying the PDI of SBMa2 should be larger than that of SBMa1, which is corresponding to the measurement results listed in Table I. On the other hand, the relative low β value also shows

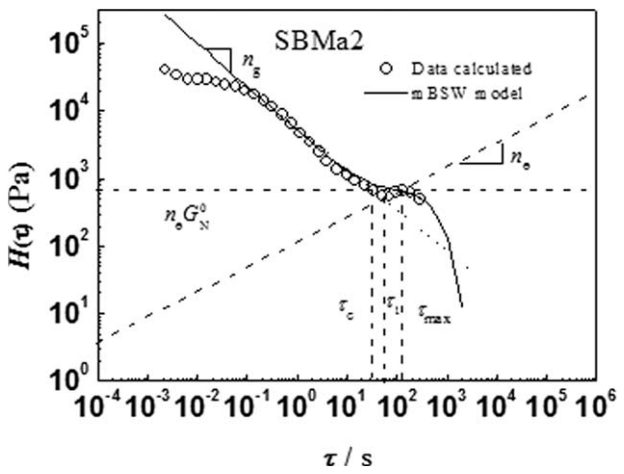

Figure 9 The relaxation time spectrum of SBMA2 and its fitting with the mBSW model.

TABLE III
The Parameters of mBSW Model for Two Block Copolymers

Samples	G_N^0 (Pa)	τ_1 (s)	τ_c (s)	τ_{max} (s)	n_e	n_g	β
SBMa2	1541	55.1	30.9	122.9	0.44	0.65	0.32
SBMa1	927	116.8	63.0	266.0	0.51	0.60	0.58

multirelaxation processes because of the relatively wide molecular weight. The τ_{max} of SBMa2 is shorter than that of SBMa1, demonstrating the long time relaxation is mainly controlled by the macromolecular chains with high molecular weight for two polymers having similar structures.

CONCLUSIONS

The viscoelastic behaviors of two SBMa block copolymers have been investigated. Curves for dynamic modulus varied with frequency (ω) show obvious solid-like behavior in the low ω region, which is corresponding to the emergence of phase separation and the relatively wide molecular weight distribution. Van Gurp–Palmen plots show two copolymers are thermorheological simple materials, exhibiting TTS is validity in the temperature windows observed. The master curves of tan δ for two copolymers show obvious valleys, which can be used to calculate $G_N^0 = 1541$ Pa (SBMa2), $G_N^0 = 927$ Pa (SBMa1). Furthermore, the curves of a_T versus T can be simulated by WLF and Arrhenius equation well, and the free volume parameters and the activation energy of two copolymers have been obtained. The relaxation time spectrums of two copolymers have been calculated according to the second differential equation of G', and the longest relaxation times have been acquired by simulating with modified mBSW model.

References

1. Nwabunma, D.; Kyu, T. Polyolefin Blends; Wiley: New Jersey, 2008.
2. Folkes, M. J; Hope, P. S. Polymer Blends and Alloys; Chapman and Hall: London, 1993.
3. Horak, Z,; Hlavata, D.; Fortelny, I.; Lednicky, F. Polym Eng Sci 2002, 42, 2042.
4. Kim, T. Y.; Kim, D. M.; Kim, W. J.; Lee, T. H.; Suh, K. S. J Polym Sci Part B: Polym Phys 2004, 42, 2813.
5. Tasdemir, M.; Karatop, S. J Appl Polym Sci 2006, 101, 559.
6. Han, C. D. Rheology in Polymer Processing; Academic Press: New York, 1976.
7. Yanovsky, Y. G. Polymer Rheology: Theory and Practice; Chapman & Hall: London, 1993.
8. Yoshida, J.; Christian, F. Macromolecules 2005, 38, 7164.
9. Chen, H. Y.; Stepanov, E. V.; Chum, S. P.; Hiltner, A.; Baer, E. J Polym Sci Part B: Polym Phys 1999, 37, 2373.
10. Chen, H. Y.; Stepanov, E. V.; Chum, S. P.; Hiltner, A.; Baer, E. Macromolecules 2000, 33, 8870.
11. Chen, H. Y.; Stepanov, E. V.; Chum, S. P.; Hiltner, A.; Baer, E. Macromolecules 1999, 32, 7587.
12. Widmaier, J. M.; Meyer, G. C. J Polym Sci Part B: Polym Phys 1980, 18, 2217.
13. Stangler, S.; Abetz, V. Rheol Acta 2003, 42, 569.
14. Thunga, M.; Staudinger, U.; Satapathy, B. K.; Weidisch, R.; Abdel-Gaod, M.; Janke, A.; Knoll, K. J Polym Sci Part B: Polym Phys 2006, 44, 2776.
15. Ferry, J. D. Viscoelastic Properties of Polymers; Wiley: New York, 1980.
16. Almdal, K.; Mortensen, K.; Ryan, A. J.; Bates, F. S. Macromolecules 1996, 29, 5940.
17. Marencic, A. P.; Wu, M. W.; Register, R. A.; Chaikin, P. M. Macromolecules 2007, 40, 7299.
18. Du, F. M.; Scogna, R. C.; Zhou, W.; Brand, S.; Fischer, J. E.; Winey, K. I. Macromolecules 2004, 37, 9048.
19. Zheng, Q.; Du, M.; Yang, B. B.; Wu, G. Polymer 2001, 42, 5743.
20. Van Gurp, M.; Palmen, J.; Proceedings of the XII International Congress on Rheology, Quebec City, Canada 1996, 134–135.
21. Van Gurp, M.; Palmen, J. Rheol Bull 1998, 67, 5.
22. Trinkle, S.; Friedrich, C. Rheol Acta 2001, 40, 322.
23. Li, R. M.; Yu, W.; Zhou, C. X. J Macromol Sci Part B: Phys 2006, 45, 889.
24. De la Fuente, J. L.; Fernández-Garciá, M.; Cerrada, M. L.; Spiess, H. W.; Wilhelm, M. Polymer 2006, 47, 1487.
25. Doi, M.; Edwards, S. F. The Theory of Polymer Dynamics; Clarendon Press: Oxford, 1986.
26. Donald, A. M.; Kramer, E. J. J Mater Sci 1982, 17, 1871.
27. Prevorsek, A. C.; De Bona, B. T. J Macromol Sci Phys B 1986, 25, 515.
28. Lomellini, P.; Rossi, A. G. Makromol Chem 1990, 191, 1729.
29. Ho, J.; Govaert, L.; Utz, M. Macromolecules 2003, 36, 7398.
30. Teerenstra, M. N.; Steeman, P. A. M.; Iwens, W.; Vandervelden, A.; Suwier, D. R.; Van Mele, B.; Koning, C. E. e-Polymers 2003, 45, 1.
31. Wu, S. J Polym Sci Polym Phys Ed 1989, 27, 723.
32. Onogi, S.; Masuda, T.; Kitagawa, K. Macromolecules 1970, 3, 109.
33. Masuda, T.; Kitagawa, K.; Inoue, T.; Onogi, S. Macromolecules 1970, 3, 116.
34. Wu, S. Polym Eng Sci 1988, 28, 538.
35. Cocchini, F.; Nobile, M. R. Rheol Acta 2003, 42, 232.
36. Nobile, M. R.; Cocchini, F. Rheol Acta 2001, 40, 111.
37. Williams, M. L.; Landel R. F.; Ferry J. D. J Am Chem Soc 1955, 77, 3701.
38. Schwarzl, F.; Staverman, A. J Appl Sci Res 1953, A4, 127.
39. Tschoegl, N. W. Rheol Acta 1971, 10, 582.
40. Tschoegl, N. W. The Theory of Linear Viscoelastic Behavior; Academic Press: New York, 1981.
41. Baumgaertel, M.; Schausberger, A.; Winter, H. H. Rheol Acta 1990, 29, 400.
42. Baumgaertel, M.; Winter, H. H. J Non-Newtonian Fluid Mech 1992, 44, 15.